

Contribution from the Department of Chemistry and Materials and Molecular Research Division, Lawrence Berkeley Laboratory, University of California, Berkeley, California 94720

A Lanthanide–Amine Template Synthesis. Preparation and Molecular Structures of $\text{Ln}(\text{L})(\text{CH}_3\text{CN})(\text{CF}_3\text{SO}_3)_3$ [$\text{L} = 1,9\text{-Bis}(2\text{-aminoethyl})\text{-}1,4,6,9,12,14\text{-hexaazacyclohexadecane}$; $\text{Ln} = \text{La, Yb}$] and $\text{La}(\text{en})_4(\text{CH}_3\text{CN})(\text{CF}_3\text{SO}_3)_3^\dagger$

PAUL H. SMITH and KENNETH N. RAYMOND*

Received February 19, 1985

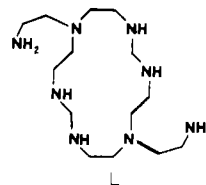
The title compounds have been prepared as part of a project to prepare kinetically inert macrocyclic amine complexes of the lanthanides in which the metal is surrounded by a covalently linked cage of amine ligating groups. The macrocycles are prepared in a reaction utilizing the metal ion as a template. The structures have been determined by single-crystal X-ray diffraction. The macrocyclic amine–lanthanide complexes have been prepared by the addition of bis(dimethylamino)methane to 1 equiv of lanthanide ion and 2 equiv of tren [$\text{N}(\text{CH}_2\text{CH}_2\text{NH}_2)_3$] in acetonitrile. The lanthanum complex ($\text{LaC}_{19}\text{H}_{39}\text{N}_9\text{O}_9\text{S}_3\text{F}_9$) prepared by this procedure is 10-coordinate with eight nitrogens from the macrocycle and two oxygens from two trifluoromethanesulfonate (triflate) anions. It crystallizes in space group $P\bar{1}$ with $Z = 2$ and $a = 10.716(2) \text{ \AA}$, $b = 13.733(2) \text{ \AA}$, $c = 14.211(2) \text{ \AA}$, $\alpha = 98.87(2)^\circ$, $\beta = 97.54(2)^\circ$, and $\gamma = 107.45(2)^\circ$. For 6711 independent data with $F_o^2 > 3\sigma(F_o^2)$, full-matrix least-squares refinement with anisotropic thermal parameters for all non-hydrogens atoms (except disordered atoms) converged to unweighted and weighted R factors of 3.92 and 6.04%, respectively. The analogous ytterbium complex ($\text{YbC}_{19}\text{H}_{39}\text{N}_9\text{O}_9\text{S}_3\text{F}_9$) is 9-coordinate with one triflate oxygen and eight nitrogens from the macrocycle. It also crystallizes in space group $P\bar{1}$ with $Z = 2$ and $a = 9.594(2) \text{ \AA}$, $b = 10.940(2) \text{ \AA}$, $c = 18.072(2) \text{ \AA}$, $\alpha = 74.07(1)^\circ$, $\beta = 74.70(1)^\circ$, and $\gamma = 81.90(1)^\circ$. For 5747 independent data a similar refinement converged to unweighted and weighted R factors of 2.49 and 2.83%, respectively. The lanthanum–ethylenediamine complex ($\text{LaC}_{13}\text{H}_{35}\text{N}_9\text{O}_9\text{S}_3\text{F}_9$) is 9-coordinate with eight nitrogens from four ethylenediamines and one oxygen from a triflate anion and crystallizes in space group $P\bar{1}$ with $Z = 2$ and $a = 9.526(2) \text{ \AA}$, $b = 12.919(2) \text{ \AA}$, $c = 14.077(2) \text{ \AA}$, $\alpha = 102.62(1)^\circ$, $\beta = 91.38(1)^\circ$, and $\gamma = 98.03(1)^\circ$. For 6124 independent data a similar refinement converged to unweighted and weighted R factors of 2.16 and 2.73%, respectively. These structures are compared, and implications are considered for the completion of a linking of the macrocycle to form a completely encapsulated lanthanide environment analogous to the sepulchrate d-transition-metal complexes.

Introduction

In addition to their thermodynamic instability with respect to most oxygen donor ligands, the lanthanide–amine complexes are solution labile. Even the neodymium complex with the tetradentate amine tren, [$\text{N}(\text{CH}_2\text{CH}_2\text{NH}_2)_3$], has been shown by NMR studies to be in equilibrium with excess free ligand in acetonitrile at room temperature.¹ We have proposed the synthesis of a kinetically inert lanthanide amine in which the metal ion is completely encapsulated in a closed macrocyclic structure. Aside from its novelty, such a complex would be an interesting candidate for a lanthanide NMR shift reagent and could have unusual electrochemical properties. Since amines have three covalent bonds in addition to their lone-pair metal binding site, their topology is ideal for the synthesis of complex polycyclic ligands. The synthesis by Sargeson and co-workers of cobalt cage complexes, the “sepulchrates”, from [$\text{Co}(\text{en})_3$]Cl₃, formaldehyde, and ammonia² is a spectacular example of this principle and suggests the use of formaldehyde as a general amine coupling reagent. With the use of a lanthanide ion as a template, one of several possible schemes would be to start with a lanthanide–amine complex and couple the individual coordinated ligands to form a macrocyclic complex. Lanthanides have been shown to be effective template ions in the formation of macrocyclic Schiff base complexes.^{3,4}

We have reported a first step in the synthesis of macrocycles based on the tetradentate ligand tren.⁵ On the basis of the interligand N–N distances in the structure of [$\text{Nd}(\text{tren})_2(\text{CH}_3\text{CN})$][ClO₄]₃, we proposed the use of propyl chains as bridging groups. However the flexibility of these complexes leaves open the possibility of utilizing shorter bridging groups, including methylene, as in the formaldehyde synthesis. The use of formaldehyde itself in the cross-linking of lanthanide–amine complexes is precluded by the production of water in the reaction. However the formaldehyde derivative bis(dimethylamino)methane, CH₂–

[N(CH₃)₂]₂, is equivalent, and we have developed a procedure for bridging NH groups of coordinated lanthanide–amine complexes. We report here the preparation and molecular structures of two methylene-bridged tren–lanthanide complexes, referred to as $\text{Ln}(\text{L})(\text{CH}_3\text{CN})(\text{CF}_3\text{SO}_3)_3$ ($\text{Ln} = \text{La, Yb}$) where $\text{L} = 1,9\text{-bis}(2\text{-aminoethyl})\text{-}1,4,6,9,12,14\text{-hexaazacyclohexadecane}$. We



have also determined the molecular structure of $\text{La}(\text{en})_4(\text{CH}_3\text{CN})(\text{CF}_3\text{SO}_3)_3$ in order to characterize the preferred geometry of this complex and the appropriate bridging units for interconnecting the ethylenediamine groups.

Experimental Section

All manipulations of moisture-sensitive compounds were accomplished with Schlenk and syringe techniques and the use of a N₂-atmosphere glovebag. Elemental analyses were performed by the Microanalytical Laboratory, University of California, Berkeley, CA. Lanthanides were determined by direct titration with EDTA with Eriochrome Black T as indicator.⁶ Infrared spectra were obtained on a Perkin-Elmer 597 spectrophotometer (Nujol mulls).

Materials. Acetonitrile was distilled from P₂O₅ immediately before use. Toluene was distilled from Na and stored over 3-Å molecular sieves

[†] This paper is dedicated to our brave friend and colleague Jean René Hamon.

* To whom correspondence should be addressed.

- (1) Johnson, M. F.; Forsberg, J. H. *Inorg. Chem.* **1972**, *11*, 2683.
- (2) Creaser, I. I.; Geue, R. J.; Harrowfield, J. M.; Herlit, A. J.; Sargeson, A. M.; Snow, M. R.; Springborg, J. *J. Am. Chem. Soc.* **1982**, *104*, 6016.
- (3) Backer-Dirks, J. D. J.; Gray, C. J.; Hart, F. A.; Hursthouse, M. B.; Schoop, B. C. *J. Chem. Soc., Chem. Commun.* **1979**, 774.
- (4) Fenton, D. E.; Casellato, U.; Vigato, P. A.; Videlli, M. *Inorg. Chim. Acta* **1984**, *95*, 187.
- (5) Eigenbrot, C. W., Jr.; Raymond, K. N. *Inorg. Chem.* **1982**, *21*, 2867; **1983**, *22*, 2972.
- (6) Flaschka, H. *Mikrochim. Acta.* **1955**, 55.

Table I. Data Collection, Solution, and Refinement Parameters for $\text{La}(\text{en})_4(\text{CH}_3\text{CN})(\text{CF}_3\text{SO}_3)_3$, $\text{La}(\text{L})(\text{CH}_3\text{CN})(\text{CF}_3\text{SO}_3)_3$, and $\text{Yb}(\text{L})(\text{CH}_3\text{CN})(\text{CF}_3\text{SO}_3)_3$

formula	$\text{LaC}_{13}\text{H}_{35}\text{N}_9\text{O}_9\text{S}_3\text{F}_9$	$\text{LaC}_{19}\text{H}_{39}\text{N}_9\text{O}_9\text{S}_3\text{F}_9$	$\text{YbC}_{19}\text{H}_{39}\text{N}_9\text{O}_9\text{S}_3\text{F}_9$
M_r	867.58	943.68	977.81
space group	$P\bar{1}$	$P\bar{1}$	$P\bar{1}$
a , Å	9.526 (2)	10.716 (2)	9.594 (2)
b , Å	12.919 (2)	13.733 (2)	10.940 (2)
c , Å	14.077 (2)	14.211 (2)	18.072 (2)
α , deg	102.62 (1)	98.87 (2)	74.068 (10)
β , deg	91.38 (1)	97.54 (2)	74.698 (13)
γ , deg	98.03 (1)	107.54 (2)	81.901 (13)
V , Å ³	1671.3 (9)	1936 (1)	1754.4 (5)
Z	2	2	2
D_{obsd} , ^a g/cm ³	1.73	1.66	1.84
D_{calcd} , g/cm ³	1.72	1.62	1.85
cryst dimens, mm	0.12 × 0.22 × 0.29 ^b	0.15 × 0.23 × 0.61 ^c	0.18 × 0.22 × 0.25 ^d
μ , cm ⁻¹	15.61	13.55	29.34
abs range T_{max}	0.844	0.999	0.999
abs range T_{min}	0.667	0.880	0.856
decay, %	10	8	20 (nonlinear)
2θ range, deg	3 < 2θ < 55	3 < 2θ < 55	3 < 2θ < 55
no. of data measd (tot)	15430	17731	16104
no. of data measd [$I > 3\sigma(I)$]	12655	13846	11944
no. of indep data (tot)	7671	8869	8052
no. of indep data [$F_o^2 > 3\sigma(F_o^2)$]	6124	6711	5747
av $R(I)$, %	1.8	1.6	2.5
av $R(F)$, %	1.4	1.5	2.0
refin R , %	2.16	3.92	2.49
refin R_w , %	2.73	6.04	2.83
GOF	0.956	1.952	0.984
p factor	0.035	0.04	0.03
no. of params	395	458	451
extcn coeff g , ^e 1/e ²	7.1×10^{-8}	2.5×10^{-7}	f
max peak on ΔF map, e/Å ³	0.29 near disordered C7	1.01 near disordered CH ₃ CN	0.65 near Yb
temp, °C	25	25	25

^a Measured by flotation in toluene/dibromomethane mixture. ^b A well-shaped parallelepiped. ^c A long wedged-shaped crystal. ^d An irregularly shaped parallelepiped. ^e Darwin, C. G. *Philos. Mag.* **1922**, *43*, 800. ^f No extinction correction was applied.

under N₂. Tren was extracted from crude triethylenetetramine⁷ and distilled from Na. Ethylenediamine was distilled from Na. Trifluoromethanesulfonic acid was used as obtained from Aldrich or Aesar. Lanthanide oxides were obtained from Brewer or Apache.

Bis(dimethylamino)methane was prepared by the addition of paraformaldehyde to an aqueous solution of dimethylamine, followed by distillation through a 1-ft Vigreux column and subsequent distillation from Na [bp 80–83 °C (1 atm), 61% yield], and it was stored under N₂. ¹H NMR (CDCl₃): δ 1.93 (s, area 2), 1.45 (s, area 6).

$\text{La}(\text{CF}_3\text{SO}_3)_3$ was prepared by the addition of trifluoromethanesulfonic acid to a suspension of La₂O₃ in water. Excess oxide was added to bring the pH to 6–7. The undissolved oxide was then removed by filtration, and the water was evaporated on a rotary evaporator. The resulting solid was dried at 160–200 °C under vacuum and used without further purification. The preparation of $\text{Yb}(\text{CF}_3\text{SO}_3)_3$ was similar except that the reaction mixture was refluxed for approximately 1 h before filtering.

$\text{La}(\text{en})_4(\text{CH}_3\text{CN})(\text{CF}_3\text{SO}_3)_3$. This preparation is analogous to the preparation of the corresponding perchlorate by Forsberg and Moeller.⁸ (**Caution!** The perchlorate compounds can result in a highly explosive material. Their use should be replaced by the procedure described here.) $\text{La}(\text{CF}_3\text{SO}_3)_3$ (2.0 g, 3.4 mmol) was weighed quickly in air and placed under N₂ in a dry Schlenk tube containing a magnetic stir bar and ~20 mL of acetonitrile. Then 1.8 mL (27 mmol) of ethylenediamine was added with stirring, and the resulting cloudy mixture was heated to reflux for ~5 min. The mixture was clarified by filtration, and the volume of the resulting clear colorless solution was reduced under vacuum to ~5 mL. When the mixture was cooled to -20 °C, a white crystalline solid formed. The complex was washed once with toluene and dried under blowing N₂ (yield 54%). The crystals used for X-ray analysis were handled in a N₂ atmosphere that was saturated with CH₃CN to prevent loss of CH₃CN from the crystal lattice. Anal. Found (calcd) for $\text{LaC}_{13}\text{H}_{35}\text{N}_9\text{O}_9\text{S}_3\text{F}_9$: La, 16.06 (16.01); C, 18.04 (18.00); H, 3.94 (4.07); N, 14.23 (14.53); S, 11.01 (11.09).

$\text{La}(\text{L})(\text{CH}_3\text{CN})(\text{CF}_3\text{SO}_3)_3$. To a suspension of $\text{La}(\text{CF}_3\text{SO}_3)_3$ (4.0 g, 6.8 mmol) in ~80 mL of acetonitrile was added tren (2.0 mL, 14 mmol).

The mixture was heated to 70–80 °C in an oil bath under N₂, and bis(dimethylamino)methane (2.8 mL, 21 mmol) was added. This mixture was stirred at 65–80 °C for approximately 8 h. The resulting slightly cloudy, yellow solution was clarified by filtration, and the acetonitrile was evaporated on a rotary evaporator to give a yellowish white solid. This crude material was recrystallized from acetonitrile by cooling a saturated solution (15–20 mL) to -20 °C. The resulting white crystalline solid was dried at room temperature under vacuum overnight (yield 78%). Crystals suitable for X-ray analysis were obtained from acetonitrile by slow cooling. Anal. Found (calcd) for $\text{LaC}_{19}\text{H}_{39}\text{N}_9\text{O}_9\text{S}_3\text{F}_9$: La, 14.97 (14.72); C, 24.76 (24.18); H, 4.39 (4.17); N, 13.60 (13.36); S, 10.24 (10.19).

$\text{Yb}(\text{L})(\text{CH}_3\text{CN})(\text{CF}_3\text{SO}_3)_3$. A mixture of $\text{Yb}(\text{CF}_3\text{SO}_3)_3$ (4.0 g, 6.5 mmol) in ~40 mL of acetonitrile was heated to 80–90 °C, and 1.9 mL (13 mmol) of tren was added. The resulting slightly cloudy mixture was refluxed under N₂ for ~24 h. The dark brown solution was evaporated under vacuum to leave a brown sticky solid, which was dried at room temperature under vacuum overnight. This solid was recrystallized once from acetonitrile/toluene and a second time from acetonitrile and was dried under blowing N₂ to give analytically pure colorless crystals (yield ~11%). Crystals suitable for X-ray analysis were obtained from an acetonitrile/toluene mixture by slow cooling and were washed with cold acetonitrile. Anal. Found (calcd) for $\text{YbC}_{19}\text{H}_{39}\text{N}_9\text{O}_9\text{S}_3\text{F}_9$: Yb, 17.76 (17.70); C, 23.50 (23.34); H, 4.08 (4.02); N, 12.89 (12.89); S, 9.84 (9.84).

Data Collection, Solution, and Refinement. All three compounds decompose readily in air; therefore, the crystals were mounted in glass capillaries in a N₂-atmosphere glovebag. The two La complexes lose their solvent of crystallization readily and were therefore mounted in a glove bag in which the N₂ atmosphere had been saturated with CH₃CN.

The following information pertains to all three structures, and details appear in Table I. Triclinic space groups were suggested by precession photographs and confirmed by successful refinements. Cell constants were determined and intensity data were collected on an Enraf-Nonius CAD-4 automated diffractometer with κ geometry using the θ - 2θ scan mode⁹ (monochromated Mo K α radiation, $\lambda = 0.71073$ Å). Data (\pm

(7) Forsberg, J. H.; Kubik, T. M.; Moeller, T.; Guwca, K. *Inorg. Chem.* **1971**, *10*, 2656.

(8) Forsberg, J. H.; Moeller, T. *Inorg. Chem.* **1969**, *8*, 883.

(9) Further details of data collection, reduction, and processing are described in: Eigenbrot, C. W., Jr.; Raymond, K. N. *Inorg. Chem.* **1982**, *21*, 2653.

Table XIV. Positional Parameters and Their Estimated Standard Deviations for $\text{La}(\text{en})_4(\text{CH}_3\text{CN})(\text{CF}_3\text{SO}_3)_3^a$

atom	<i>x</i>	<i>y</i>	<i>z</i>	<i>B</i> , Å ²
La	0.25364 (1)	0.16392 (1)	0.31190 (1)	2.178 (2)
S1	0.25718 (6)	-0.07140 (5)	0.44706 (5)	3.14 (1)
S2	-0.20644 (7)	0.38407 (5)	0.37777 (5)	3.64 (1)
S3	0.1337 (1)	0.21055 (7)	-0.04919 (6)	5.59 (2)
F1	0.3544 (3)	-0.2141 (2)	0.3168 (2)	9.14 (6)
F2	0.1369 (3)	-0.2056 (2)	0.2927 (2)	9.81 (6)
F3	0.2051 (3)	-0.2793 (1)	0.4035 (2)	8.57 (7)
F4	-0.0765 (2)	0.5664 (2)	0.3544 (2)	8.30 (7)
F5	-0.2694 (2)	0.5112 (2)	0.2685 (2)	7.06 (5)
F6	-0.0839 (2)	0.4386 (2)	0.2291 (2)	7.61 (5)
F7	0.2958 (4)	0.2172 (3)	-0.1929 (2)	14.0 (1)
F8	0.3574 (4)	0.3392 (3)	-0.0635 (3)	16.1 (1)
F9	0.1836 (5)	0.3486 (2)	-0.1527 (2)	16.8 (1)
O1	0.2980 (2)	0.0038 (1)	0.3870 (1)	3.82 (4)
O2	0.1186 (2)	-0.0641 (2)	0.4826 (2)	4.87 (5)
O3	0.3626 (2)	-0.0787 (2)	0.5170 (2)	4.91 (5)
O4	-0.2959 (2)	0.2991 (2)	0.3123 (2)	5.56 (5)
O5	-0.0738 (2)	0.3560 (2)	0.4043 (2)	5.39 (5)
O6	-0.2795 (2)	0.4418 (2)	0.4542 (2)	5.76 (5)
O7	0.1016 (4)	0.2920 (2)	0.0294 (2)	8.52 (8)
O8	0.2187 (4)	0.1393 (2)	-0.0198 (2)	9.15 (8)
O9	0.0190 (3)	0.1597 (2)	-0.1169 (2)	8.11 (7)
N1	0.0089 (2)	0.0276 (2)	0.3043 (1)	3.19 (4)
N2	0.0288 (2)	0.2049 (2)	0.2137 (2)	3.42 (4)
N3	0.5012 (2)	0.0923 (2)	0.2638 (2)	3.35 (4)
N4	0.2460 (2)	0.0208 (2)	0.1392 (2)	3.72 (5)
N5	0.1448 (2)	0.2132 (2)	0.4876 (2)	3.97 (5)
N6	0.4447 (2)	0.2493 (2)	0.4623 (2)	3.58 (5)
N7	0.2421 (2)	0.3799 (2)	0.3586 (2)	3.93 (5)
N8	0.3820 (2)	0.2837 (2)	0.1934 (2)	4.25 (5)
N9	0.3438 (5)	0.7331 (4)	0.9392 (4)	12.2 (2)
C1	-0.1186 (3)	0.0659 (2)	0.2721 (2)	3.97 (6)
C2	-0.0877 (3)	0.1141 (2)	0.1859 (2)	3.99 (6)
C3	0.5029 (5)	0.0379 (4)	0.1586 (3)	4.04 (9)*
C3'	0.4880 (7)	-0.0027 (5)	0.1831 (5)	3.8 (1)*
C4	0.3698 (5)	-0.0395 (4)	0.1296 (3)	4.16 (9)*
C4'	0.3930 (7)	0.0102 (5)	0.1025 (5)	3.8 (1)*
C5	0.2502 (3)	0.2277 (2)	0.5691 (2)	4.45 (7)
C6	0.3831 (3)	0.2964 (2)	0.5538 (2)	4.19 (6)
C7	0.3574 (5)	0.4423 (4)	0.3142 (4)	4.2 (1)*
C7'	0.2707 (7)	0.4346 (5)	0.2777 (5)	4.5 (1)*
C8	0.3752 (4)	0.3978 (3)	0.2187 (3)	7.23 (9)
C9	0.2816 (5)	0.6784 (4)	0.9851 (4)	9.9 (2)
C10	0.1991 (7)	0.6116 (5)	1.0421 (5)	12.5 (2)
C11	0.2347 (4)	-0.1994 (2)	0.3607 (2)	5.18 (7)
C12	-0.1567 (3)	0.4797 (2)	0.3036 (2)	4.91 (7)
C13	0.2492 (6)	0.2825 (4)	-0.1169 (3)	9.4 (1)

^aStarred values indicate atoms were refined with isotropic thermal parameters. Anisotropically refined atoms are given in the form of the isotropic equivalent thermal parameter defined as $\frac{1}{3}[a^2B(1,1) + b^2B(2,2) + c^2B(3,3) + ab(\cos \gamma)B(1,2) + ac(\cos \beta)B(1,3) + bc(\cos \alpha)B(2,3)]$.

h, ±k, ±l were collected while three intensity standards were monitored every 2 h of X-ray exposure time and three orientation standards were checked every 250 reflections. The structures were solved by using heavy-atom techniques. Hydrogens were placed in idealized positions, with isotropic thermal parameters based on their parent carbon and nitrogen atoms, and were not refined. The acetonitrile hydrogens were not included. Full-matrix least-squares refinements were employed by using the reflections with $F_o^2 > 3\sigma(F_o^2)$. Atomic scattering factors were taken from ref 10. Structure factors, rms vibrational amplitudes, anisotropic thermal parameters, and hydrogen atom coordinates are available as supplementary material (Tables II–XIII).¹¹

Results

Syntheses. The synthesis of the $\text{Ln}(\text{L})(\text{trif})_3$ complexes was accomplished by the reaction of 2 equiv of tren with bis(dimethylamino)methane (mn) in the presence of 1 equiv of the

Table XV. Intramolecular Distances (Å) and Angles (deg) for $\text{La}(\text{en})_4(\text{CH}_3\text{CN})(\text{CF}_3\text{SO}_3)_3$

La–O1	2.598 (2)	La–N5	2.687 (2)
La–N1	2.703 (2)	La–N6	2.692 (2)
La–N2	2.697 (2)	La–N7	2.741 (2)
La–N3	2.699 (2)	La–N8	2.715 (2)
La–N4	2.707 (2)		
S1–O1	1.442 (2)	S1–O3	1.417 (2)
S1–O2	1.431 (2)	S1–C11	1.809 (3)
N1–C1	1.472 (3)	N5–C5	1.469 (4)
N2–C2	1.476 (4)	N6–C6	1.472 (4)
N3–C3	1.496 (6)	N7–C7	1.501 (6)
N3–C3'	1.468 (8)	N7–C7'	1.478 (8)
N4–C4	1.495 (5)	N8–C8	1.450 (4)
N4–C4'	1.517 (7)		
C1–C2	1.498 (4)	C7'–C8	1.381 (8)
C3–C4	1.488 (7)	C9–C10	1.466 (9)
C3'–C4'	1.487 (1)	C11–F1	1.326 (4)
C5–C6	1.490 (4)	C11–F2	1.301 (4)
C7–C8	1.366 (7)	C11–F3	1.306 (4)
O1–La–N1	70.07 (6)	N2–La–N6	142.88 (7)
O1–La–N2	133.13 (6)	N2–La–N7	70.70 (7)
O1–La–N3	66.60 (6)	N2–La–N8	78.23 (7)
O1–La–N4	84.56 (7)	N3–La–N4	64.40 (7)
O1–La–N5	77.64 (7)	N3–La–N5	129.52 (7)
O1–La–N6	74.90 (7)	N3–La–N6	72.28 (7)
O1–La–N7	142.73 (7)	N3–La–N7	120.10 (7)
O1–La–N8	138.83 (7)	N3–La–N8	72.24 (7)
N1–La–N2	63.52 (6)	N4–La–N5	146.96 (7)
N1–La–N3	121.66 (6)	N4–La–N6	136.52 (7)
N1–La–N4	74.53 (7)	N4–La–N7	132.45 (7)
N1–La–N5	73.31 (7)	N4–La–N8	77.00 (8)
N1–La–N6	129.63 (7)	N5–La–N6	64.58 (7)
N1–La–N7	118.12 (7)	N5–La–N7	71.36 (7)
N1–La–N8	136.13 (7)	N5–La–N8	133.40 (7)
N2–La–N3	135.74 (7)	N6–La–N7	73.43 (7)
N2–La–N4	77.46 (7)	N6–La–N8	93.80 (8)
N2–La–N5	94.71 (7)	N7–La–N8	62.78 (7)
O1–S1–O2	112.55 (12)	O2–S1–O3	115.19 (14)
O1–S1–O3	115.52 (12)	O2–S1–C11	103.72 (16)
O1–S1–C11	102.93 (15)	O3–S1–C11	104.99 (15)
La–O1–S1	151.45 (11)		
La–N1–C1	114.98 (15)	La–N5–C5	113.31 (17)
La–N2–C2	114.69 (15)	La–N6–C6	114.54 (16)
La–N3–C3	113.43 (22)	La–N7–C7	112.10 (25)
La–N3–C3'	114.6 (3)	La–N7–C7'	114.5 (3)
La–N4–C4	112.97 (23)	La–N8–C8	116.79 (20)
La–N4–C4'	112.4 (3)		
N1–C1–C2	109.79 (21)	N7–C7'–C8	114.4 (5)
N2–C2–C1	109.14 (22)	N8–C8–C7	117.1 (4)
N3–C3–C4	109.2 (4)	N8–C8–C7'	119.1 (4)
N3–C3'–C4'	110.2 (6)	S1–C11–F1	110.4 (3)
N4–C4–C3	109.0 (4)	S1–C11–F2	111.91 (24)
N4–C4'–C3'	109.2 (6)	S1–C11–F3	111.7 (3)
N5–C5–C6	111.10 (23)	F1–C11–F2	107.1 (3)
N6–C6–C5	110.80 (23)	F1–C11–F3	106.0 (3)
N7–C7–C8	113.8 (4)	F2–C11–F3	109.5 (3)

lanthanide triflate salt in acetonitrile. The reaction mixture was heated in order to increase the rate and to drive off the dimethylamine as it was formed. The product was isolated by crystallization.

The advantages of using this particular formaldehyde derivative as a coupling reagent are fourfold: (1) The reaction of this compound with an amine produces dimethylamine, which is volatile and eventually leaves the reaction mixture as a gas, thereby driving the reaction toward the desired product. (2) The reaction does not produce water, which reacts with lanthanide amine complexes to form insoluble lanthanide hydroxides. (3) Imine or Schiff base reactions are in general reversible, which may allow this reaction to proceed to the thermodynamically stable product, thereby decreasing the number of possible isomers or alternative products. (4) The small bite angle of the N–CH₂–N moiety favors

(10) "International Tables for X-Ray Crystallography"; Kynoch Press: Birmingham, England, 1974; Vol. 4, Tables 2.2b and 2.3.1.

(11) Supplementary material; for ordering information see the statement at the end of this paper.

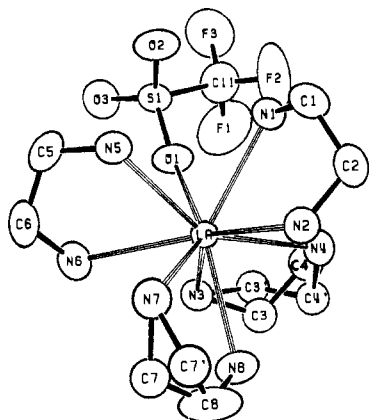


Figure 1. ORTEP drawing of $[\text{La}(\text{en})_4(\text{CF}_3\text{SO}_3)]^{2+}$ drawn with 50% probability ellipsoids and the crystallographic numbering scheme.

high coordination numbers around the metal.

Structure of $\text{La}(\text{en})_4(\text{CH}_3\text{CN})(\text{CF}_3\text{SO}_3)_3$. The structure of the $\text{La}(\text{en})_4(\text{CF}_3\text{SO}_3)^{2+}$ cation is shown in Figure 1 along with the crystallographic numbering scheme. A stereoview is illustrated in Figure 2. The refined positional parameters appear in Table XIV, and the bond distances and angles for the cation appear in Table XV. The lanthanum ion is coordinated to four bidentate ethylenediamine ligands and one triflate oxygen making it 9-coordinate. Two of the ethylenediamine ligands have a conformational disorder (δ to λ) in the ethylene bridge, as shown in Figures 1 and 2; the occupancies of the disordered atoms, C3, C4 and C3', C4', were assigned as 60 and 40%, and those of C7 and C7', were assigned as 55 and 45%, respectively. The occupancies assigned were based on an iterative procedure, which minimized the differences between the thermal parameters. The large thermal ellipsoid of C8 is also presumed to be due to an unresolved disorder. The coordination geometry can be described as a distorted tricapped trigonal prism (Figure 3). The pertinent dihedral angles compare well with those calculated for an idealized tricapped trigonal prism¹² (Table XVI).¹¹

The La-N bond lengths range from 2.692 (2) to 2.741 (2) Å with an average of 2.705 Å, and the average ethylenediamine bite angle is 63.8°, ranging from 62.8 to 64.6°. The intraligand N-N distances range from 2.842 (3) to 2.881 (3) Å with an average of 2.860 Å. The shortest interligand N-N distances are between 3.15 and 3.41 Å, giving some indication of the preferred ligand-ligand distances for 9-coordinate lanthanum. The NH groups are hydrogen bonded to seven triflate oxygens (Figure 4¹¹) with N-O distances ranging from 3.000 (4) to 3.215 (3) Å. The unit cell packing diagram is illustrated in Figure 5.¹¹

Structure of $\text{La}(\text{L})(\text{CH}_3\text{CN})(\text{CF}_3\text{SO}_3)_3$. The positional parameters are listed in Table XVII, and the intramolecular distances and angles for $\text{La}(\text{L})(\text{CF}_3\text{SO}_3)_2^+$ are listed in Table XVIII. The numbering scheme is illustrated in Figure 6, and the stereoview shown in Figure 7. The 10-coordinate lanthanum ion includes eight amine nitrogens from L and two oxygens from two triflate anions. If one ignores the orientation of the triflate anions, the complex has a noncrystallographic C_2 axis passing through the La ion and bisecting the O1-La-O4 angle. This twofold axis was analyzed by defining a C_2 rotation axis and calculating the differences between the new and old atom positions after rotation. The axis was defined as the vector from La to a point X, obtained by the summation of the midpoints between all pseudo-twofold-related atoms. The results are listed in Table XIX.¹¹ The largest difference is for the two oxygen atoms at 0.12 Å. The average differences (and esd's) are 0.061 (14) Å for the nitrogen atoms and 0.056 (24) Å for the carbon atoms. The overall average difference is 0.063 (27) Å.

The coordination geometry is not highly regular, but can be viewed as a distorted bicapped square antiprism (BSAP) in which

Table XVII. Positional Parameters and Their Estimated Standard Deviations for $\text{La}(\text{L})(\text{CH}_3\text{CN})(\text{CF}_3\text{SO}_3)_3^a$

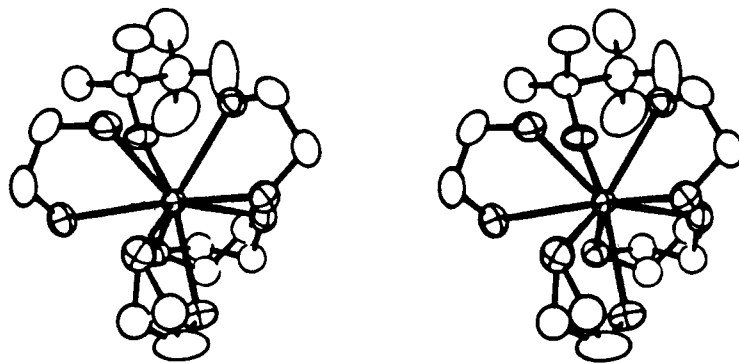
atom	x	y	z	B, Å ²
La	0.17651 (3)	0.32837 (2)	0.19364 (2)	3.034 (5)
S1	-0.1411 (1)	0.0801 (1)	0.1039 (1)	5.88 (4)
S2	0.2046 (2)	0.5895 (1)	0.0981 (1)	4.89 (3)
S3	0.6054 (1)	0.2738 (1)	0.4594 (1)	5.17 (3)
F1	-0.3984 (4)	0.0052 (4)	0.0746 (4)	11.2 (2)
F2	-0.3060 (5)	0.0999 (6)	0.2126 (4)	16.6 (2)
F3	-0.3101 (5)	0.1771 (4)	0.0950 (7)	16.3 (3)
F4	0.4533 (4)	0.7034 (4)	0.1457 (3)	9.1 (1)
F5	0.3420 (5)	0.7152 (3)	0.2587 (3)	8.5 (1)
F6	0.3166 (6)	0.7904 (3)	0.1403 (4)	11.3 (2)
F7	0.6848 (5)	0.1167 (3)	0.4195 (5)	12.0 (2)
F8	0.5861 (7)	0.1150 (4)	0.5350 (4)	13.3 (2)
F9	0.4752 (6)	0.0804 (4)	0.3881 (5)	14.1 (2)
O1	-0.0473 (3)	0.1782 (3)	0.1616 (3)	4.73 (9)
O2	-0.1456 (5)	0.0709 (5)	0.0054 (4)	11.6 (2)
O3	-0.1373 (5)	-0.0078 (4)	0.1408 (7)	14.5 (3)
O4	0.2393 (3)	0.5080 (3)	0.1374 (3)	4.50 (8)
O5	0.2157 (6)	0.5881 (4)	0.0004 (3)	8.1 (1)
O6	0.0855 (4)	0.6041 (4)	0.1249 (4)	8.0 (1)
O7	0.4943 (5)	0.2856 (5)	0.4966 (6)	11.5 (2)
O8	0.6022 (6)	0.2874 (4)	0.3643 (4)	10.1 (2)
O9	0.7272 (4)	0.3248 (3)	0.5241 (3)	5.8 (1)
N1	0.3451 (4)	0.3214 (3)	0.0586 (3)	3.96 (9)
N2	0.0596 (4)	0.2908 (4)	0.0082 (3)	4.8 (1)
N3	0.4470 (4)	0.4067 (3)	0.2627 (3)	3.79 (9)
N4	0.2158 (4)	0.1431 (3)	0.1435 (3)	4.3 (1)
N5	0.0740 (4)	0.3287 (3)	0.3661 (3)	4.5 (1)
N6	-0.0274 (4)	0.4028 (3)	0.1986 (4)	5.0 (1)
N7	0.3139 (4)	0.4872 (3)	0.3417 (3)	3.81 (9)
N8	0.2378 (4)	0.2028 (3)	0.3131 (3)	4.4 (1)
N9	0.25102 (2)	0.29872 (4)	0.67908 (2)	10.7 (3)*
N9'	0.18765 (2)	0.31925 (1)	0.69372 (1)	10.7*
C1	0.2786 (6)	0.3337 (5)	-0.0357 (4)	5.1 (1)
C2	0.1382 (6)	0.2654 (5)	-0.0633 (4)	5.7 (1)
C3	0.4709 (5)	0.4123 (4)	0.0938 (4)	4.8 (1)
C4	0.5395 (5)	0.4149 (4)	0.1925 (4)	4.7 (1)
C5	0.3759 (5)	0.2204 (4)	0.0450 (4)	4.6 (1)
C6	0.3543 (5)	0.1642 (4)	0.1266 (4)	4.5 (1)
C7	-0.0562 (6)	0.3471 (5)	0.3498 (4)	5.7 (2)
C8	-0.0540 (6)	0.4307 (5)	0.2971 (5)	5.7 (1)
C9	0.1664 (6)	0.4117 (5)	0.4479 (4)	4.9 (1)
C10	0.3076 (6)	0.4472 (4)	0.4322 (4)	4.5 (1)
C11	0.0535 (6)	0.2233 (5)	0.3901 (4)	5.4 (1)
C12	0.1744 (6)	0.1914 (4)	0.3981 (4)	5.5 (1)
C13	0.4424 (5)	0.5073 (4)	0.3130 (4)	4.0 (1)
C14	0.2003 (6)	0.1092 (4)	0.2368 (4)	5.0 (1)
C15	-0.2962 (7)	0.0934 (7)	0.1211 (6)	8.3 (2)
C16	0.3363 (7)	0.7062 (5)	0.1644 (5)	6.5 (2)
C17	0.5855 (8)	0.1404 (5)	0.4489 (6)	7.6 (2)
C18	-0.27134 (1)	0.21977 (3)	0.67308 (1)	6.0 (3)*
C18'	0.06243 (1)	0	0	13.4 (7)*
C19	0.27866 (2)	0.1149 (1)	0.65438 (3)	8.0 (4)
C19'	-0.07500 (1)	0.21028 (1)	0.65910 (1)	13.7 (6)

^a See footnote a in Table XIV.

one triflate oxygen and four nitrogens from L (the nitrogens from each original tren ligand) make up each of the two eclipsed square pyramids. The tertiary nitrogens, N1 and N5, form the caps of the square antiprism. The polyhedron is illustrated in Figure 8. The dihedral angles are listed in Table XX¹¹ along with those calculated for an idealized BSAP¹³ for comparison. The La-N bond lengths range from 2.669 (4) to 2.816 (3) Å with an average of 2.734 Å. The N-La-N angles for the ethylene-bridged nitrogens range from 62.50 (10) to 64.66 (10)° and average 63.90°; the bite angles for the methylene-bridged nitrogens are 51.02 (10) and 51.80 (9)°. The average N-N distances for the ethylene- and methylene-bridged nitrogens are 2.92 and 2.36 Å, respectively. The closest nonbridged N-N distances are N2-N6 and N3-N8 at 3.29 and 3.27 Å, respectively. The ligand is hydrogen bonded to six triflate oxygens (Figure 9¹¹) with N-O distances ranging

(12) Guggenberger, L. J.; Muetterties, E. L. *J. Am. Chem. Soc.* **1976**, *98*, 7221.

(13) Robertson, B. E. *Inorg. Chem.* **1977**, *16*, 2735.

Figure 2. Stereoscopic ORTEP drawing of $[\text{La}(\text{en})_4(\text{CF}_3\text{SO}_3)]^{2+}$.Table XVIII. Intramolecular Distances (Å) and Angles (deg) for $\text{La}(\text{L})(\text{CH}_3\text{CN})(\text{CF}_3\text{SO}_3)_3$

La–O1	2.585 (3)	La–N4	2.701 (3)	C1–C2	1.479 (7)	C15–F1	1.369 (6)
La–O4	2.632 (3)	La–N5	2.816 (3)	C3–C4	1.487 (6)	C15–F2	1.311 (8)
La–N1	2.814 (3)	La–N6	2.677 (3)	C5–C6	1.495 (6)	C15–F3	1.303 (9)
La–N2	2.669 (4)	La–N7	2.685 (3)	C7–C8	1.460 (6)	C16–F4	1.325 (6)
La–N3	2.756 (3)	La–N8	2.751 (3)	C9–C10	1.503 (6)	C16–F5	1.321 (6)
N1–C1	1.493 (6)	N5–C7	1.486 (5)	C11–C12	1.481 (6)	C16–F6	1.320 (6)
N1–C3	1.500 (6)	N5–C9	1.499 (5)	S1–O1	1.460 (3)	S2–O4	1.444 (3)
N1–C5	1.509 (6)	N5–C11	1.497 (5)	S1–O2	1.381 (5)	S2–O5	1.409 (4)
N2–C2	1.468 (6)	N6–C8	1.481 (6)	S1–O3	1.397 (5)	S2–O6	1.439 (4)
N3–C4	1.491 (6)	N7–C10	1.478 (5)	S1–C15	1.769 (6)	S2–C16	1.812 (6)
N3–C13	1.471 (6)	N7–C13	1.447 (6)				
N4–C6	1.484 (6)	N8–C12	1.470 (6)				
N4–C14	1.487 (5)	N8–C14	1.461 (5)				
O1–La–O4	130.78 (9)	N1–La–N8	102.65 (10)	La–O1–S1	151.14 (18)	La–O4–S2	152.16 (17)
O1–La–N1	117.29 (9)	N2–La–N3	125.30 (10)	La–N1–C1	108.51 (23)	La–N5–C7	109.14 (21)
O1–La–N2	70.09 (10)	N2–La–N4	84.31 (9)	La–N1–C3	108.24 (22)	La–N5–C9	111.71 (22)
O1–La–N3	150.43 (9)	N2–La–N5	132.16 (10)	La–N1–C5	111.72 (22)	La–N5–C11	107.54 (22)
O1–La–N4	70.01 (9)	N2–La–N6	75.84 (10)	C1–N1–C3	108.1 (3)	C7–N5–C9	109.0 (3)
O1–La–N5	71.39 (9)	N2–La–N7	141.05 (10)	C1–N1–C5	109.8 (3)	C7–N5–C11	109.2 (3)
O1–La–N6	69.00 (10)	N2–La–N8	133.15 (10)	C3–N1–C5	110.4 (3)	C9–N5–C11	110.2 (3)
O1–La–N7	135.43 (10)	N3–La–N4	85.60 (9)	La–N2–C2	115.8 (3)	La–N6–C8	114.23 (22)
O1–La–N8	78.94 (9)	N3–La–N5	102.05 (9)	La–N3–C4	119.11 (23)	La–N7–C10	107.87 (22)
O4–La–N1	71.98 (9)	N3–La–N6	135.50 (10)	La–N3–C13	93.8 (3)	La–N7–C13	97.39 (24)
O4–La–N2	72.90 (10)	N3–La–N7	51.02 (10)	C4–N3–C13	114.6 (3)	C10–N7–C13	113.8 (3)
O4–La–N3	78.52 (9)	N3–La–N8	72.75 (9)	La–N4–C6	107.98 (21)	La–N8–C12	119.17 (23)
O4–La–N4	136.31 (9)	N4–La–N5	107.85 (9)	La–N4–C14	96.83 (24)	La–N8–C14	95.0 (23)
O4–La–N5	115.16 (9)	N4–La–N6	138.46 (10)	C6–N4–C14	111.8 (3)	C12–N8–C14	115.9 (3)
O4–La–N6	71.37 (10)	N4–La–N7	128.24 (9)	N1–C1–C2	112.1 (4)	N4–C14–N8	107.8 (3)
O4–La–N7	68.48 (9)	N4–La–N8	51.80 (9)	N2–C2–C1	111.3 (4)	S1–C15–F1	110.7 (5)
O4–La–N8	149.50 (8)	N5–La–N6	64.54 (10)	N1–C3–C4	113.3 (4)	S1–C15–F2	110.3 (5)
N1–La–N2	64.66 (10)	N5–La–N7	64.34 (10)	N3–C4–C3	111.4 (4)	S1–C15–F3	111.2 (5)
N1–La–N3	62.50 (10)	N5–La–N8	62.64 (9)	N1–C5–C6	113.9 (3)	F1–C15–F2	103.9 (6)
N1–La–N4	64.59 (10)	N6–La–N7	87.12 (10)	N4–C6–C5	111.1 (3)	F1–C15–F3	112.4 (6)
N1–La–N5	162.35 (9)	N6–La–N8	124.38 (10)	N5–C7–C8	112.7 (3)	F2–C15–F3	108.1 (7)
N1–La–N6	132.13 (10)	N7–La–N8	85.32 (9)	N6–C8–C7	110.6 (4)	S2–C16–F4	110.5 (4)
N1–La–N7	106.74 (10)			N5–C9–C10	113.1 (3)	S2–C16–F5	111.1 (4)
O1–S1–O2	113.77 (24)	O4–S2–O5	114.73 (22)	N7–C10–C9	110.4 (3)	S2–C16–F6	110.8 (4)
O1–S1–O3	114.2 (3)	O4–S2–O6	112.90 (20)	N5–C11–C12	114.2 (3)	F4–C16–F5	107.8 (5)
O1–S1–C15	102.10 (23)	O4–S2–C16	102.60 (21)	N8–C12–C11	111.9 (3)	F4–C1–F6	108.5 (5)
O2–S1–O3	115.9 (4)	O5–S2–O6	116.2 (3)	N3–C13–N7	106.8 (3)	F5–C16–F6	108.0 (5)
O2–S1–C15	104.3 (3)	O5–S2–C16	104.3 (3)				
O3–S1–C15	104.4 (4)	O6–S2–C16	104.0 (3)				

from 2.982 (5) to 3.165 (5) Å. The unit cell packing diagram is illustrated in Figure 10.^{11,14}

Structure of $\text{Yb}(\text{L})(\text{CH}_3\text{CN})(\text{CF}_3\text{SO}_3)_3$. The $\text{Yb}(\text{L})(\text{CF}_3\text{SO}_3)_3^{2+}$ cation is illustrated in Figure 11 with the crystallographic numbering scheme, and a stereoview is shown in Figure 12. The

positional parameters are listed in Table XXI, and the intramolecular distances and angles for the cation are listed in Table XXII. The coordination geometry can be described as a monocapped square antiprism and is illustrated in Figure 13. The pertinent dihedral angles are listed in Table XVI¹¹ along with the idealized angles for this geometry.¹²

The Yb–N bond lengths range from 2.442 (3) to 2.611 (3) Å with an average of 2.523 Å. The ethylene-bridged N–La–N angles range from 66.61 (11) to 69.87 (10)° with an average bite angle of 68.02°. The methylene-bridged N–La–N angles are 55.05 (10) and 55.20 (9)°. The average N–N distances for the ethylene- and methylene-bridged nitrogens are 2.85 and 2.35 Å, respectively. The closest nonbridged N–N distances are N2–N6 [3.051 (4) Å], N3–N6 [3.085 (6) Å], and N7–N8 [3.042 (4) Å]. The ligand

(14) The unit cell diagram illustrates an acetonitrile that is disordered. On the basis of difference Fourier maps, a model is proposed in which two acetonitrile molecules labeled C19–C18–N9 and C19'–C18'–N9' were assigned 50% occupancies. They were refined as two units with C18–N9 and C18–C19 distances constrained to 1.170 (5) and 1.470 (5) Å, respectively, and the C19–C18–N9 angles constrained to 180.0 (6)°. The N9–N9' distance was also constrained to 0.750 (5) Å. Only C19 and C19' were refined anisotropically. [Note: Two low-angle reflections (1,–1,0 and 0,2,–1) with very large $w\Delta F^2$ values were rejected.]

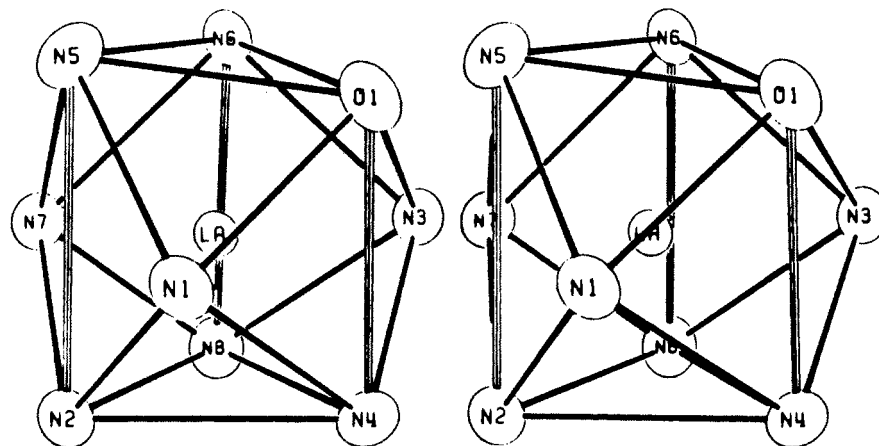


Figure 3. Stereoview of the coordination geometry for $[\text{La}(\text{en})_4(\text{CF}_3\text{SO}_3)_2]^+$.

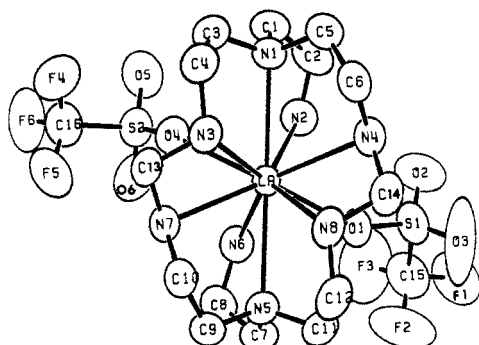


Figure 6. ORTEP drawing of $[\text{La}(\text{L})(\text{CF}_3\text{SO}_2)_2]^+$ drawn with 50% probability ellipsoids and the crystallographic numbering scheme.

is hydrogen bonded to five different triflate oxygens (Figure 14¹¹) with N–O distances ranging from 2.987 (4) to 3.205 (5) Å. The unit cell packing diagram is illustrated in Figure 15.¹¹

Discussion

Three important comparisons can be drawn from this study. First, the two lanthanum structures allow the comparison of the simple unconstrained $\text{La}(\text{en})_4^{3+}$ system to the somewhat more constrained $\text{La}(\text{L})^{3+}$ system. Second, the role of the metal in determining the macrocyclic ligand structure can be evaluated by comparing $\text{La}(\text{L})^{3+}$ to $\text{Yb}(\text{L})^{3+}$. Third, a comparison of the two 9-coordinate species, $\text{La}(\text{en})_4^{3+}$ and $\text{Yb}(\text{L})^{3+}$, can give some insight into structural preferences for 9-coordination.

There is a significant difference in the range of La–N bond lengths within the two lanthanum species. The La–N range ($\text{La}-\text{N}_{\text{max}} - \text{La}-\text{N}_{\text{min}}$) is 0.049 Å for $\text{La}(\text{en})_4^{3+}$ and 0.147 Å for $\text{La}(\text{L})^{3+}$, indicating the constraints placed on the system by the extra N–N connections in the latter. For comparison the range of Nd–N bonds in $\text{Nd}(\text{tren})_2^{3+}$ is 0.11 Å,⁵ representing a system that is intermediate between these two extremes. A comparison between the average bite angles of the nitrogens connected by ethylene units in the two systems, 63.8° for $\text{La}(\text{en})_4^{3+}$ and 63.9°

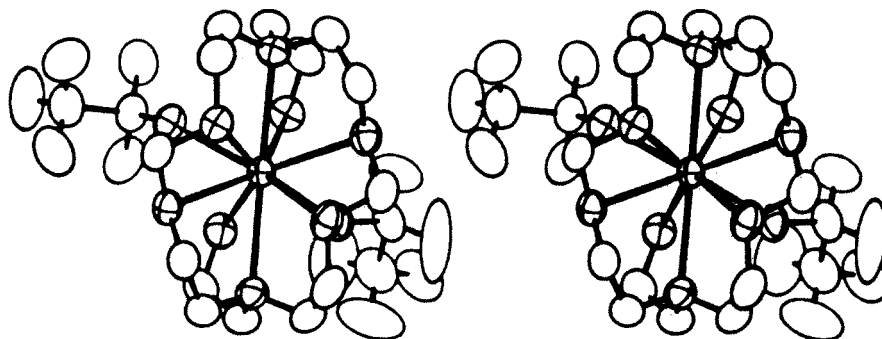


Figure 7. Stereoscopic ORTEP drawing of $[\text{La}(\text{L})(\text{CF}_3\text{SO}_2)_2]^+$.

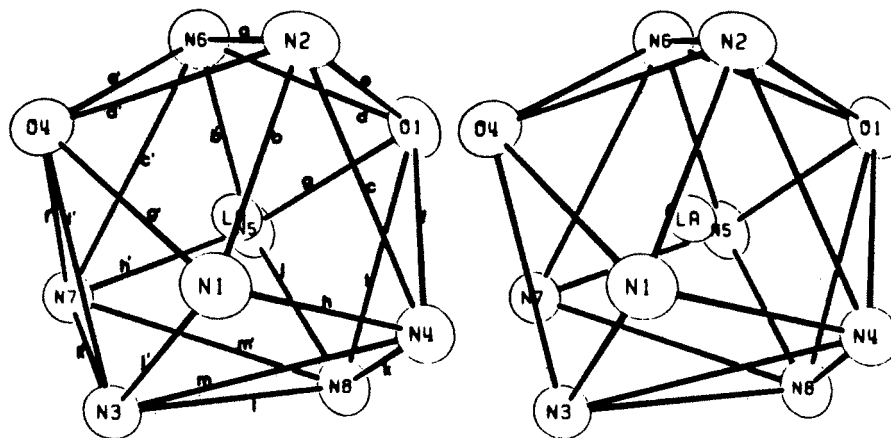


Figure 8. Stereoview of the coordination geometry for $[\text{La}(\text{L})(\text{CF}_3\text{SO}_2)_2]^+$.

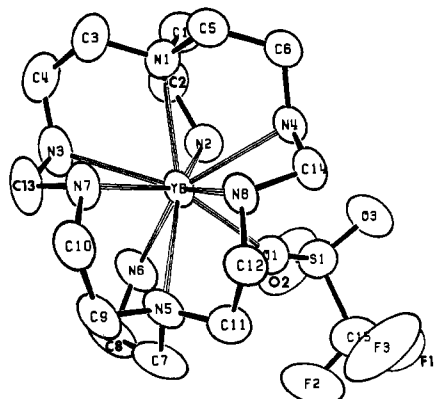


Figure 11. ORTEP drawing of $[\text{Yb}(\text{L})(\text{CF}_3\text{SO}_3)]^{2p}$ drawn with 50% probability ellipsoids and the crystallographic numbering scheme.

Table XXI. Positional Parameters and Their Estimated Standard Deviations for $\text{Yb}(\text{L})(\text{CH}_3\text{CN})(\text{CF}_3\text{SO}_3)_2^a$

atom	x	y	z	B, Å ²
Yb	0.12285 (2)	0.36098 (1)	0.24368 (1)	3.041 (3)
S1	-0.0891 (1)	0.2346 (1)	0.14461 (6)	4.75 (2)
S2	0.3025 (1)	0.7894 (1)	0.50537 (6)	6.22 (3)
S3	0.4006 (1)	0.36966 (9)	0.85166 (6)	4.12 (2)
F1	-0.1405 (3)	0.0761 (3)	0.0738 (2)	9.57 (9)
F2	-0.0119 (4)	-0.0017 (3)	0.1543 (2)	13.3 (1)
F3	0.0756 (4)	0.1179 (4)	0.0456 (2)	14.3 (1)
F4	0.5456 (3)	0.6880 (3)	0.4392 (3)	11.6 (1)
F5	0.3704 (4)	0.5712 (3)	0.4726 (3)	12.1 (1)
F6	0.3834 (5)	0.7311 (4)	0.3721 (2)	13.3 (1)
F7	0.3613 (4)	0.1579 (3)	0.8248 (2)	11.9 (1)
F8	0.5635 (4)	0.1597 (3)	0.8507 (3)	12.0 (1)
F9	0.3714 (4)	0.1420 (3)	0.9430 (2)	11.8 (1)
O1	0.0380 (3)	0.2497 (2)	0.1692 (1)	4.23 (6)
O2	-0.2057 (4)	0.1951 (4)	0.2094 (2)	10.7 (1)
O3	-0.1183 (4)	0.3348 (3)	0.0824 (2)	10.8 (1)
O4	0.3441 (4)	0.9150 (3)	0.4624 (2)	7.1 (1)
O5	0.1564 (4)	0.7666 (5)	0.5110 (2)	10.4 (1)
O6	0.3431 (4)	0.7431 (4)	0.5786 (2)	9.4 (1)
O7	0.4752 (3)	0.3959 (3)	0.9036 (2)	5.22 (7)
O8	0.4695 (3)	0.4138 (3)	0.7694 (2)	6.63 (9)
O9	0.2473 (3)	0.3940 (3)	0.8720 (2)	5.92 (8)
N1	0.0746 (3)	0.5930 (3)	0.2532 (2)	3.81 (7)
N2	-0.1376 (3)	0.4181 (3)	0.2752 (2)	4.18 (7)
N3	0.1121 (3)	0.3883 (4)	0.3842 (2)	5.00 (9)
N4	0.0993 (3)	0.5164 (3)	0.1115 (2)	3.55 (7)
N5	0.3067 (3)	0.1631 (3)	0.2324 (2)	4.12 (7)
N6	0.0251 (3)	0.1655 (3)	0.3360 (2)	5.00 (8)
N7	0.3359 (3)	0.3684 (3)	0.2942 (2)	4.26 (8)
N8	0.3223 (3)	0.4051 (3)	0.1231 (2)	3.49 (7)
N9	0.1402 (5)	0.2072 (5)	0.5601 (3)	9.2 (2)
C1	-0.0844 (4)	0.6306 (4)	0.2694 (2)	4.6 (1)
C2	-0.1777 (4)	0.5234 (4)	0.3151 (2)	4.8 (1)
C3	0.1342 (4)	0.6153 (4)	0.3158 (2)	5.1 (1)
C4	0.0873 (5)	0.5190 (4)	0.3945 (2)	5.6 (1)
C5	0.1502 (4)	0.6726 (3)	0.1760 (2)	4.28 (9)
C6	0.1035 (4)	0.6537 (3)	0.1072 (2)	4.26 (9)
C7	0.2268 (4)	0.0452 (4)	0.2691 (3)	5.8 (1)
C8	0.1263 (5)	0.0500 (4)	0.3467 (3)	6.4 (1)
C9	0.4243 (4)	0.1548 (4)	0.2729 (2)	4.9 (1)
C10	0.4657 (4)	0.2822 (4)	0.2751 (2)	4.8 (1)
C11	0.3662 (4)	0.1728 (4)	0.1465 (2)	4.6 (1)
C12	0.4278 (4)	0.2984 (4)	0.1024 (2)	4.27 (9)
C13	0.2630 (5)	0.3378 (5)	0.3792 (2)	5.6 (1)
C14	0.2310 (4)	0.4603 (4)	0.0662 (2)	3.99 (9)
C15	-0.0399 (5)	0.1010 (4)	0.1016 (3)	6.6 (1)
C16	0.4065 (6)	0.6888 (5)	0.4437 (4)	7.8 (2)
C17	0.4249 (5)	0.1978 (5)	0.8692 (3)	7.4 (2)
C18	0.2179 (5)	0.1328 (5)	0.5884 (3)	6.4 (1)
C19	0.3174 (6)	0.0403 (5)	0.6254 (4)	8.1 (2)

^a See footnote a in Table XIV.

for $\text{La}(\text{L})^{3+}$, suggests that these bite angles are not particularly sensitive to these constraints. The average N–N distances for the ethylene-bridged nitrogens are also similar, 2.86 Å for $\text{La}(\text{en})_4^{3+}$

Table XXII. Intramolecular Distances (Å) and Angles (deg) for $\text{Yb}(\text{L})(\text{CH}_3\text{CN})(\text{CF}_3\text{SO}_3)_2$

Yb–O1	2.390 (3)	Yb–N5	2.611 (3)
Yb–N1	2.559 (3)	Yb–N6	2.453 (3)
Yb–N2	2.442 (3)	Yb–N7	2.468 (3)
Yb–N3	2.611 (4)	Yb–N8	2.475 (3)
Yb–N4	2.568 (3)		
N1–C1	1.495 (5)	N5–C7	1.494 (5)
N1–C3	1.483 (5)	N5–C9	1.478 (6)
N1–C5	1.486 (5)	N5–C11	1.486 (5)
N2–C2	1.475 (5)	N6–C8	1.481 (6)
N3–C4	1.470 (6)	N7–C10	1.476 (5)
N3–C13	1.464 (5)	N7–C13	1.476 (5)
N4–C6	1.489 (5)	N8–C12	1.495 (5)
N4–C14	1.468 (5)	N8–C14	1.475 (4)
C1–C2	1.494 (6)	C11–C12	1.500 (6)
C3–C4	1.520 (6)	C15–F1	1.290 (6)
C5–C6	1.500 (6)	C15–F2	1.304 (7)
C7–C8	1.487 (7)	C15–F3	1.285 (7)
C9–C10	1.516 (6)		
S1–O1	1.448 (3)	S1–O3	1.395 (4)
S1–O2	1.405 (4)	S1–C15	1.788 (6)
O1–Yb–N1	131.11 (9)	N2–Yb–N6	77.10 (10)
O1–Yb–N2	78.05 (10)	N2–Yb–N7	138.47 (11)
O1–Yb–N3	146.12 (10)	N2–Yb–N8	135.29 (10)
O1–Yb–N4	71.61 (9)	N3–Yb–N4	134.09 (11)
O1–Yb–N5	74.15 (10)	N3–Yb–N5	103.39 (11)
O1–Yb–N6	72.78 (11)	N3–Yb–N6	75.00 (12)
O1–Yb–N7	141.38 (10)	N3–Yb–N7	55.05 (10)
O1–Yb–N8	82.79 (9)	N3–Yb–N8	128.41 (10)
N1–Yb–N2	69.87 (10)	N4–Yb–N5	115.42 (10)
N1–Yb–N3	66.61 (11)	N4–Yb–N6	140.97 (11)
N1–Yb–N4	67.49 (10)	N4–Yb–N7	118.12 (10)
N1–Yb–N5	148.77 (10)	N4–Yb–N8	55.20 (9)
N1–Yb–N6	130.63 (11)	N5–Yb–N6	68.50 (10)
N1–Yb–N7	83.07 (11)	N5–Yb–N7	68.05 (11)
N1–Yb–N8	94.75 (10)	N5–Yb–N8	67.62 (9)
N2–Yb–N3	84.88 (11)	N6–Yb–N7	99.69 (11)
N2–Yb–N4	80.40 (10)	N6–Yb–N8	134.04 (11)
N2–Yb–N5	140.69 (11)	N7–Yb–N8	75.97 (10)
O1–S1–O2	112.20 (23)	O2–S1–O3	117.3 (3)
O1–S1–O3	113.01 (24)	O2–S1–C15	104.0 (3)
O1–S1–C15	104.79 (22)	O3–S1–C15	103.8 (3)
Yb–O1–S1	142.91 (17)	Yb–N1–C3	112.04 (24)
Yb–N1–C1	110.61 (23)	Yb–N1–C5	106.98 (22)
C1–N1–C3	109.1 (3)	Yb–N5–C11	106.59 (21)
C1–N1–C5	110.3 (3)	C7–N5–C9	108.1 (3)
C3–N1–C5	107.8 (3)	C7–N5–C11	109.3 (4)
Yb–N2–C2	113.23 (24)	C9–N5–C11	110.9 (3)
Yb–N3–C4	116.99 (25)	Yb–N6–C8	117.46 (24)
Yb–N3–C13	91.57 (23)	Yb–N7–C10	119.0 (3)
C4–N3–C13	112.6 (4)	Yb–N7–C13	97.09 (23)
Yb–N4–C6	115.60 (22)	C10–N7–C13	112.9 (3)
Yb–N4–C14	93.36 (19)	Yb–N8–C12	119.46 (21)
C6–N4–C14	114.4 (3)	Yb–N8–C14	97.04 (19)
Yb–N5–C7	108.66 (23)	C12–N8–C14	114.0 (3)
Yb–N5–C9	113.2 (3)		
N1–C1–C2	114.4 (3)	N5–C11–C12	112.9 (3)
N2–C2–C1	109.0 (3)	N8–C12–C11	110.0 (3)
N1–C3–C4	112.0 (4)	N3–C13–N7	106.2 (3)
N3–C4–C3	110.9 (3)	N4–C14–N8	105.2 (3)
N1–C5–C6	112.8 (3)	S1–C15–F1	113.2 (4)
N4–C6–C5	112.1 (3)	S1–C15–F2	110.6 (5)
N5–C7–C8	111.9 (4)	S1–C15–F3	111.4 (4)
N6–C8–C7	109.3 (3)	F1–C15–F2	106.7 (5)
N5–C9–C10	114.7 (3)	F1–C15–F3	108.1 (6)
N7–C10–C9	111.2 (3)	F2–C15–F3	106.5 (5)

and 2.92 Å for $\text{La}(\text{L})^{3+}$. The fact that $\text{La}(\text{L})^{3+}$ is 10-coordinate and $\text{La}(\text{en})_4^{3+}$ is 9-coordinate illustrates the effect of the small N–CH₂–N bite angles in the former, which allows more room at the metal for an extra triflate anion.

The Ln–N ranges for the two $\text{Ln}(\text{L})^{3+}$ complexes are quite similar [0.147 Å for $\text{La}(\text{L})^{3+}$ and 0.169 Å for $\text{Yb}(\text{L})^{3+}$]. The

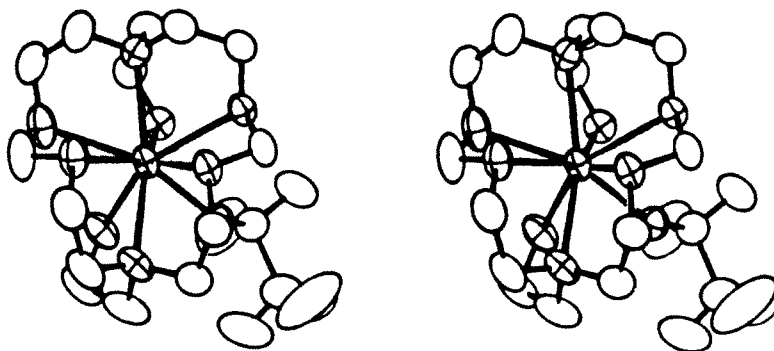


Figure 12. Stereoscopic ORTEP drawing of $[\text{Yb}(\text{L})(\text{CF}_3\text{SO}_3)]^{2+}$.

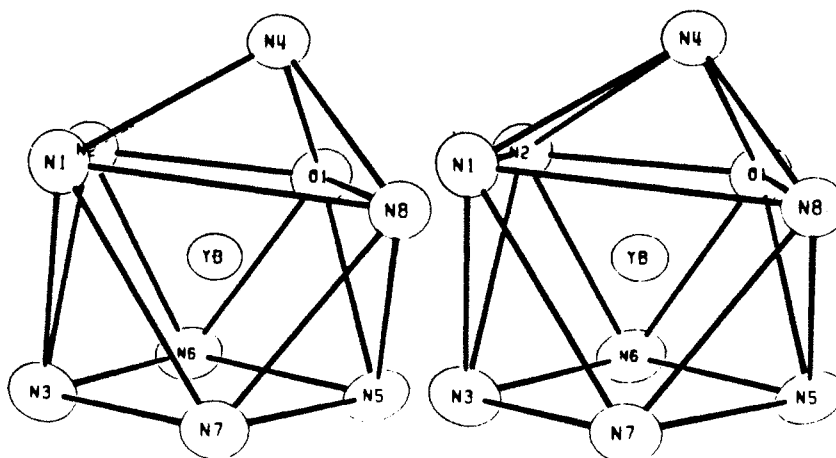


Figure 13. Stereoview of the coordination geometry for $[\text{Yb}(\text{L})(\text{CF}_3\text{SO}_3)]^{2+}$.

slightly larger range for the Yb complex may be indicative of increased intraligand N–N repulsions due to the shorter Yb–N distances. The average ethylene-bridged N–Yb–N bite angle of 68.0° is somewhat larger than the 63.9° angle of the $\text{La}(\text{L})^{3+}$ cation, but this difference can be attributed to the shortening of the Ln–N bond lengths in going from La to Yb. The average N–N distances for the ethylene-bridged nitrogens are 2.92 and 2.85 Å for $\text{La}(\text{L})^{3+}$ and $\text{Yb}(\text{L})^{3+}$, respectively. The larger methylene-bridged N–Yb–N angles (55.1 and 55.2°) compared to those in $\text{La}(\text{L})^{3+}$ (51.0 and 51.8°) are again indicative of the shorter Yb–N bond lengths. The average methylene-bridged N–N distances are quite similar, i.e. 2.36 Å for $\text{La}(\text{L})^{3+}$ and 2.35 Å for $\text{Yb}(\text{L})^{3+}$. The decrease in coordination number from 10 to 9 in going from La^{3+} to Yb^{3+} we ascribe to the smaller size of Yb^{3+} (~ 0.2 Å difference).

It is interesting to note the relative conformations of the hexaaza macrocycles in these two complexes (Figures 7 and 12). In the lanthanum species the macrocycle is somewhat "closed" in comparison to the "open" conformation of the macrocycle in the ytterbium species. This difference is illustrated by the difference in the N1–Ln–N5 angles of 162.4 and 148.8° for the La and Yb species, respectively. In the ytterbium species it appears that if the conformation of the macrocycle were to adapt the conformation seen in the lanthanum species, the formation of a third methylene bridge would be facilitated. This difference in macrocycle conformation may be due to the change in coordination number around the metal.

Finally, a comparison of the two 9-coordinate complexes is warranted. The small angle (0.5°) (Table XVI)¹¹ between the planes N3–N6–N7 and N5–N6–N7 in the $\text{Yb}(\text{L})^{3+}$ polyhedron distinguishes it as a monocapped square antiprism. The smallest corresponding angle (21.0°) (Table XVI)¹¹ in the $\text{La}(\text{en})_4^{3+}$ complex illustrates that the coordination geometry is closer to a tricapped trigonal prism. It is clear that the extra N–N connections in $\text{Yb}(\text{L})^{3+}$ have distorted the geometry significantly from the more common tricapped-trigonal-prism geometry seen in the $\text{La}(\text{en})_4(\text{CF}_3\text{SO}_3)^{2+}$ cation. The effect of metal size on the geometry is presumed to be small.

The structures presented here are self-consistent. They allow the analysis of ligand constraint, metal size, and 9-coordinate geometry. On the basis of the above discussion, we suggest that the possibility exists for forming a third methylene bridge in the ytterbium species, and we are attempting this. We also suggest the possibility of connecting N2 to N6 in $\text{La}(\text{L})(\text{CF}_3\text{SO}_3)_3$ with an ethylene unit by using 1,2-dibromoethane as the coupling reagent.

Acknowledgment. We thank Dr. Steven Rodgers for helpful discussions and the generous gift of the tren ligand, Gwen Freeman for her help with the lanthanide titrations, and Dr. F. J. Hollander for his assistance with the structure solutions, which were completed on the CHEXRAY facility (partially supported by the NSF). This work was supported by the Director, Office of Energy Research, Office of Basic Energy Sciences, Chemical Sciences Division of the U.S. Department of Energy, under Contract No. DE-AC03-76SF00098.

Registry No. $\text{La}(\text{en})_4(\text{CH}_3\text{CN})(\text{CF}_3\text{SO}_3)_3$, 98064-69-8; $\text{La}(\text{L})(\text{CH}_3\text{CN})(\text{CF}_3\text{SO}_3)_3$ (L = 1,9-bis(2-aminoethyl)-1,4,6,9,12,14-hexaazacyclohexadecane), 98087-73-1; $\text{Yb}(\text{L})(\text{CH}_3\text{CN})(\text{CF}_3\text{SO}_3)_3$ (L = 1,9-bis(2-aminoethyl)-1,4,6,9,12,14-hexaazacyclohexadecane), 98104-55-3; tren, 4097-89-6; bis(dimethylamino)methane, 51-80-9.

Supplementary Material Available: Table II [values of $10F_o$ and $10F_c$ for $\text{La}(\text{en})_4(\text{CH}_3\text{CN})(\text{CF}_3\text{SO}_3)_3$], Table III [root-mean-square amplitudes of thermal vibration (Å) for $\text{La}(\text{en})_4(\text{CH}_3\text{CN})(\text{CF}_3\text{SO}_3)_3$], Table IV [temperature factor expressions (B 's) for $\text{La}(\text{en})_4(\text{CH}_3\text{CN})(\text{CF}_3\text{SO}_3)_3$], Table V [calculated hydrogen atom positional parameters for $\text{La}(\text{en})_4(\text{CH}_3\text{CN})(\text{CF}_3\text{SO}_3)_3$], Table VI [values of $10F_o$ and $10F_c$ for $\text{La}(\text{L})(\text{CH}_3\text{CN})(\text{CF}_3\text{SO}_3)_3$], Table VII [root-mean-square amplitudes of thermal vibration (Å) for $\text{La}(\text{L})(\text{CH}_3\text{CN})(\text{CF}_3\text{SO}_3)_3$], Table VIII [temperature factor expressions (B 's) for $\text{La}(\text{L})(\text{CH}_3\text{CN})(\text{CF}_3\text{SO}_3)_3$], Table IX [calculated hydrogen atom positional parameters for $\text{La}(\text{L})(\text{CH}_3\text{CN})(\text{CF}_3\text{SO}_3)_3$], Table X [values of $10F_o$ and $10F_c$ for $\text{Yb}(\text{L})(\text{CH}_3\text{CN})(\text{CF}_3\text{SO}_3)_3$], Table XI [root-mean-square amplitudes of thermal vibration (Å) for $\text{Yb}(\text{L})(\text{CH}_3\text{CN})(\text{CF}_3\text{SO}_3)_3$], Table XII [temperature factor expressions (B 's) for $\text{Yb}(\text{L})(\text{CH}_3\text{CN})(\text{CF}_3\text{SO}_3)_3$], Table XIII [calculated hydrogen atom positional parameters for $\text{Yb}(\text{L})(\text{CH}_3\text{CN})(\text{CF}_3\text{SO}_3)_3$], Table XVI [polyhedral angles for $\text{La}(\text{en})_4(\text{CF}_3\text{SO}_3)^{2+}$ and $\text{Yb}(\text{L})(\text{CF}_3\text{SO}_3)^{2+}$], Table XIX [results of a twofold

rotation on $\text{La}(\text{L})(\text{CF}_3\text{SO}_3)_2^+$, Table XX [polyhedral angles for $\text{La}(\text{L})(\text{CF}_3\text{SO}_3)_2^+$], Figure 4 [stereoview of the hydrogen bonding around $[\text{La}(\text{en})_4(\text{CF}_3\text{SO}_3)_2]^{2+}$], Figure 5 [stereoview of the unit cell packing diagram for $\text{La}(\text{en})_4(\text{CH}_3\text{CN})(\text{CF}_3\text{SO}_3)_3$], Figure 9 [stereoview of the hydrogen bonding around $[\text{La}(\text{L})(\text{CF}_3\text{SO}_3)_2]^+$], Figure 10 [stereoview

of the unit cell packing diagram for $\text{La}(\text{L})(\text{CH}_3\text{CN})(\text{CF}_3\text{SO}_3)_3$], Figure 14 [stereoview of the hydrogen bonding around $[\text{Yb}(\text{L})(\text{CF}_3\text{SO}_3)_2]^{2+}$], and Figure 15 [stereoview of the unit cell packing diagram for $\text{Yb}(\text{L})(\text{CH}_3\text{CN})(\text{CF}_3\text{SO}_3)_3$] (156 pages). Ordering information is given on any current masthead page.

Contribution from the Department of Chemistry,
The University of Michigan, Ann Arbor, Michigan 48109

Tertiary Alkylphosphine Adducts of $\text{Mo}_2(\text{O}_2\text{CCF}_3)_4$ ($\text{Mo}-\text{Mo}$)¹

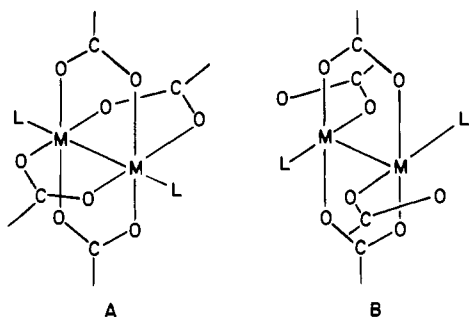
D. J. SANTURE and A. P. SATTELBERGER*²

Received September 5, 1984

$\text{Mo}_2(\text{O}_2\text{CCF}_3)_4$ reacts with 2 equiv of PR_3 ($\text{R} = \text{Me}, \text{Et}, n\text{-Bu}$) in toluene to give adducts of stoichiometry $\text{Mo}_2(\text{O}_2\text{CCF}_3)_4 \cdot 2\text{PR}_3$. These complexes have been characterized by solid-state infrared spectroscopy and variable-temperature ^{19}F and $^{31}\text{P}\{^1\text{H}\}$ NMR. A single isomer, with equatorially bound phosphines, is observed in solution at temperatures below ca. -40°C in each case. Previous work on the PMe_3 and PEt_3 adducts suggested that there were two or more equatorial isomers present in solution at low temperature. The discrepancy between the two studies can be traced to the purity of $\text{Mo}_2(\text{O}_2\text{CCF}_3)_4$, which is usually prepared by metathesis of $\text{Mo}_2(\text{O}_2\text{CCH}_3)_4$ in refluxing trifluoroacetic acid. In our hands, this procedure gives a product contaminated with $\text{Mo}_2(\text{O}_2\text{C}-\text{CF}_3)_3(\text{O}_2\text{CCH}_3)$. X-ray structural studies on $\text{Mo}_2(\text{O}_2\text{CCF}_3)_4 \cdot 2\text{PBu}_3$ show that this complex has a C_{2h} core, which is presumably maintained in solution. The Mo-Mo and Mo-P bond lengths are 2.105 (1) and 2.542 (2) Å, respectively. The differences in solution behavior between homologous $\text{M}_2(\text{O}_2\text{CCF}_3)_4 \cdot 2\text{PR}_3$ complexes ($\text{M} = \text{Mo}, \text{W}$) are discussed and correlated with M-P bond strengths. Phosphine-exchange reactions are used to generate the mixed-phosphine equatorial adducts $\text{M}_2(\text{O}_2\text{CCF}_3)_4 \cdot \text{PEt}_3 \cdot \text{PBu}_3$ ($\text{M} = \text{Mo}, \text{W}$) in solution. The electronic absorption spectra of $\text{M}_2(\text{O}_2\text{CCF}_3)_4 \cdot 2\text{PMe}_3$ ($\text{M} = \text{Mo}, \text{W}$) are reported and the $\delta \rightarrow \delta^*$, $^1\text{A}_g \rightarrow ^1\text{B}_u$ transitions are assigned and discussed. Crystal data (at -125°C) for $\text{Mo}_2(\text{O}_2\text{CCF}_3)_4 \cdot 2\text{PBu}_3$ are as follows: monoclinic space group $I2/a$, $a = 19.390$ (10) Å, $b = 10.414$ (4) Å, $c = 21.790$ (11) Å, $\beta = 94.64$ (4)°, $V = 4385.58$ Å³, $Z = 4$, $d_{\text{calcd}} = 1.586$ g cm⁻³.

Introduction

There are several reports in the literature on the reactions of tetrakis(trifluoroacetato)dimolybdenum(II), $\text{Mo}_2(\text{TFA})_4$, with tertiary phosphines,³⁻⁵ and two general classes of $\text{Mo}_2(\text{TFA})_4 \cdot 2\text{PR}_3$ complexes have been isolated and characterized by IR, NMR, and X-ray crystallography. The class I complexes, obtained with bulky phosphines, are simple axial adducts (A). Two members



of this class have been examined crystallographically,^{4,5} and both have rather long Mo-P bonds (>2.96 Å), implying only a weak interaction. Not surprisingly, these adducts are extensively dissociated in solution.³

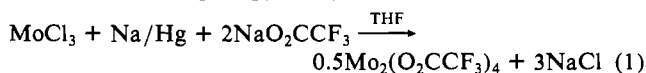
The reactions of $\text{Mo}_2(\text{TFA})_4$ with small, basic tertiary phosphines, e.g., triethylphosphine, provide class II complexes. In these, one equatorially bound oxygen on each of two trifluoroacetate ligands is displaced by a phosphine. Six geometrical isomers are possible for an $\text{Mo}_2(\text{TFA})_4 \cdot 2\text{PR}_3$ dimer³ containing only one pair of bidentate CF_3CO_2^- ligands, and one of these (the C_{2h} isomer) is shown (B). Two members of this class have also been studied by X-ray crystallography.⁴ A C_{2h} core structure was found for both, and the Mo-P bonds (2.51–2.53 Å) were appreciably shorter

than those found in the class I structures. The solution behavior of several class II compounds has been examined by variable-temperature $^{31}\text{P}\{^1\text{H}\}$ and ^{19}F NMR spectroscopy and was not amenable to any simple interpretation.³ At least two equatorial isomers were observed in CDCl_3 solutions of the class II complexes, and their stereochemistry could not be determined by spectroscopic techniques.³

In a recent paper,⁶ we described the syntheses and physicochemical properties of several class II phosphine adducts of tetrakis(trifluoroacetato)ditungsten(II). We found that a single equatorial isomer was present in solutions of $\text{W}_2(\text{TFA})_4 \cdot 2\text{PR}_3$ ($\text{R} = \text{Me}, \text{Et}, n\text{-Bu}$), as judged by variable-temperature ^{19}F and $^{31}\text{P}\{^1\text{H}\}$ NMR spectroscopy. Furthermore, a comparison of the solid-state and solution infrared spectra, coupled with the crystal structure of $\text{W}_2(\text{TFA})_4 \cdot 2\text{PBu}_3$, a C_{2h} isomer, led us to conclude that the solution and solid-state structures of each complex were identical. We then speculated that the differences in solution behavior between homologous $\text{M}_2(\text{TFA})_4 \cdot 2\text{PR}_3$ complexes were a reflection of the differences in M-P bond strengths, i.e., $\text{W-P} > \text{Mo-P}$. However, it was not clear what connection, if any, there was between weak Mo-P bonds and the observation of multiple equatorial isomers in solution. As a consequence, we decided to reinvestigate the solution behavior of several class II phosphine adducts of $\text{Mo}_2(\text{TFA})_4$. Our results, which differ from those reported earlier,³ are described herein together with the X-ray structure of $\text{Mo}_2(\text{TFA})_4 \cdot 2\text{PBu}_3$.

Results and Discussion

Synthesis of $\text{Mo}_2(\text{TFA})_4$. The $\text{Mo}_2(\text{TFA})_4$ used in our studies was prepared by a route that is quite different than the one described in the literature.⁷ Polymeric molybdenum trichloride was reduced in THF with sodium amalgam in the presence of 2 equiv of sodium trifluoroacetate to provide dark yellow-brown solutions containing $\text{Mo}_2(\text{TFA})_4$ (reaction 1). After filtration,



solvent removal, and sublimation (100°C , 10^{-5} torr) of the brown

(1) Metal-Metal Bonded Complexes of the Early Transition Metals. 10. Part 9: Santure, D. J.; Huffman, J. C.; Sattelberger, A. P. *Inorg. Chem.* **1985**, *24*, 371.

(2) Present address: Los Alamos National Laboratory, INC-4, Mail Stop C345, Los Alamos, NM 87545.

(3) Girolami, G. S.; Mainz, V. V.; Andersen, R. A. *Inorg. Chem.* **1980**, *19*, 805.

(4) Cotton, F. A.; Lay, D. G. *Inorg. Chem.* **1981**, *20*, 935.

(5) Girolami, G. S.; Andersen, R. A. *Inorg. Chem.* **1982**, *21*, 1318.

(6) Santure, D. J.; Huffman, J. C.; Sattelberger, A. P. *Inorg. Chem.* **1984**, *23*, 938.

(7) Cotton, F. A.; Norman, J. G., Jr. *J. Coord. Chem.* **1971**, *1*, 161.